Cosmogenic Activation Calculation of Experiments using Liquid Argon Targets

Teena Vallivilayil John[a)]

Gran Sasso Science Institute, Viale Francesco Crispi, 7, 67100 L'Aquila, Italy
on behalf of the DarkSide Collaboration

[a)]*Corresponding author: teena.vallivilayil@gssi.it*

Abstract. Rare-event search experiments need extremely low backgrounds. The cosmogenic background of detector materials affects the sensitivity of the experiments, so its estimation before the detector installation is necessary. Many upcoming experiments, including the DarkSide-20k (DS-20k) WIMP-search experiment, use liquid argon (LAr) as a target. The dominant radioactive isotopes produced in LAr include ^{3}H, ^{37}Ar, ^{39}Ar, and ^{42}Ar. DS-20k will use Underground Argon (UAr) as the target, which will be transported from its extraction site in Colorado to the detector site in Italy. We developed an Activation Calculation Software tool to estimate the induced activity of radioactive isotopes produced during UAr transportation. The software helps us to efficiently plan the ^{39}Ar depletion required for LAr experiments. A comparison with measurements from the DarkSide-50 experiment is left for future work.

OVERVIEW

The detection of rare events demands an ultra-low background condition. Cosmic rays and their secondaries are an important background source in rare-event search experiments. The installation of a detector in deep underground laboratories with passive and active shields limits the background from cosmic rays and other radiation at the Earth's surface. However, radioisotopes produced by cosmogenic activation of detector materials during their manufacturing, transport, and storage can cause significant backgrounds that limit sensitivity. Therefore, determining the cosmogenic activation of detector materials before installation is necessary.

Liquid Argon (LAr) is planned as a target for many future experiments, including DarkSide-20k (DS-20k). DS-20k is a planned experiment searching for WIMPs with a dual-phase TPC filled with 50 tons of Underground Argon (UAr). It will be installed at Laboratori Nazionali del Gran Sasso (LNGS), Italy, under 1440 meter water equivalent of rock. The dominant radioactive isotopes produced in LAr include ^{3}H, ^{37}Ar, ^{39}Ar, and ^{42}Ar [1]. Due to its long half-life and the difficulty separating it from ^{40}Ar, ^{39}Ar is especially important for experiments looking for nuclear-recoil signals below 565 keV, while ^{42}Ar may pose a background to MeV-scale rare-event searches. In experiments looking for a rare event like DS-20k, the presence of ^{39}Ar can lead to a high rate of decay, which causes a large signal-pileup fraction and high dead time and, thereby, limits the sensitivity. Atmospheric argon (AAr) has a specific activity of 1 Bq/kg for ^{39}Ar, and DarkSide-50 (DS-50) measured a specific activity of 7.4×10^{-4} Bq/kg in UAr [2]. DS-20k is designed to have an ultra-low background rate of 0.1 neutron-induced nuclear recoils in 10 yr. The projected 90% CL sensitivity of DS-20k to spin-independent WIMP-nucleon scattering cross-sections is 1×10^{-47} cm^{2} for a WIMP of 1 TeV/c^{2} of mass [3, 4]. The estimation of the cosmogenic background activated during UAr transportation will help us to plan the required ^{39}Ar depletion and thereby achieve the projected sensitivity.

The ^{39}Ar contamination may be further reduced through isotopic distillation with the Aria facility [5]. Aria is a cryogenic distillation plant designed to produce rare, stable isotopes. It can deplete ^{39}Ar in UAr by a factor of 10 per pass. Besides ^{39}Ar, the cosmogenic activation of other radioactive isotopes may pose a significant contribution to the total activity, and achieving high radiopurity requires transportation and storage plans that account for the activation of the target in transit and storage. The UAr used for the DS-50 experiment was transported from Colorado, USA, to LNGS, Italy. We developed an Activation Calculation Software tool to estimate the induced activity of radioactive isotopes produced whilst the UAr was being transported. The estimate will be compared to DS-50 data in the future. Once validated, the Activation Calculation tool will be used to estimate the induced activity of radioisotopes in UAr of DS-20k, helping us to efficiently plan the ^{39}Ar depletion required for DS-20k UAr.

RADIOACTIVE ISOTOPES IN ARGON

The interaction of cosmic-ray particles with ^{40}Ar produces ^{37}Ar and ^{39}Ar. Thermal-neutron interaction with ^{36}Ar produces ^{37}Ar, and ^{3}H can be produced from the fast-neutron interaction with all Ar stable isotopes. The involved processes are

$$
\begin{aligned}
&{}^{40}Ar+n \rightarrow^{37} Ar+4n, \qquad\qquad {}^{36}Ar+n \rightarrow^{37} Ar \\
&{}^{40}Ar+n \rightarrow^{3} H+^{38}Cl, \quad {}^{38}Ar+n \rightarrow^{3} H+^{36}Cl, \quad {}^{36}Ar+n \rightarrow^{3} H+^{34}Cl.
\end{aligned} \tag{1}
$$

^{37}Ar decays by electron capture resulting in the emission of Auger electrons from the K (2.38 keV) and L1 (0.277 keV) atomic shells. ^{3}H decays by beta emission with an endpoint energy of 18 keV. Even though ^{37}Ar does not pose a significant background in the WIMP search, it provides a valuable calibration at low activities. It provides a useful benchmark for these calculations.

DS-20k is looking for high-mass WIMPs, which will produce nuclear recoils with energy between $30-200$ keV. Because of the pulse-shape discrimination, the isotopes of Ar will not be a significant background to the high-mass WIMP search. However, they can induce a high event rate that might result in higher dead time in the experiment. We will use the induced activity of ^{37}Ar from DS-50 data to validate the results of the Activation Calculation tool, as it has a half-life of 35 d which is shorter than those of the other isotopes considered here.

SOFTWARE PACKAGE

We developed a software package for evaluating the activation of radioisotopes in UAr and AAr. It is based on a compiled selection of reaction cross-section measurements and models, the PARMA [6] and Gordon [7] flux models, and the user-specified transportation history and initial composition of the target argon. The code is designed to be flexible and easily extensible. The flux and reaction cross-section models can easily be changed, different cross-section estimates and scaling factors can be used over different energy ranges, and the capabilities for calculating the activation of other target materials may be added in the future. The software package is written in the C++ programming language.

Software framework

The Activation Calculation Software package contains five subroutines—Flux, Cross-section, History, Config, and Activation. The config file specifies the configuration parameters, such as the isotopic composition of the target, the set of reactions to include in the calculation, and the dataset used for reaction cross-sections and projectile fluxes. The software can also take multiple datasets for a particular reaction. The Config subroutine will read the config file containing the input information. The History subroutine will get the transportation history of UAr. The Flux subroutine will choose a model for the flux calculation. The software package needs a detailed transportation history, including latitude, longitude, altitude, and a timestamp. Based on the input transportation data, the flux subroutine will estimate the flux of projectiles at each location. The cross-section subroutine will get the production cross-sections from the cross-section libraries. The reaction cross-sections of ^{37}Ar and ^{3}H are added to the cross-section library. Based on specified reaction options in the config file, the cross-section subroutine will give the cross-section as a function of projectile energy. Finally, the activation subroutine will take the flux and cross-section as an input and compute the activation. The activation of each radioisotope R is the integral of the product of the flux and reaction cross-section over the full spectrum. The radioisotope causes induced activity (IA) during the exposure period:

$$
R=\int f(E)\sigma(E)dE, \quad IA=R(1-e^{-\lambda t_{\mathrm{exp}}})e^{-\lambda t_{\mathrm{cool}}}, \tag{2}
$$

where t_{exp} represents the exposure time, i.e., the time when UAr is exposed at a fixed location, t_{cool} represents the cooling time, i.e., the time between when the UAr is exposed and when the detector starts running, and λ represents the decay constant of the radioisotope. We integrate over the transportation history to estimate the total induced activity during the UAr transportation.

Flux Libraries

The software offers two options to estimate the flux based on the location and timestamp details: the EXPAC simulation [8] and the Gordon model [7]. EXPAC is software based on the PARMA model. The PARMA model comprises

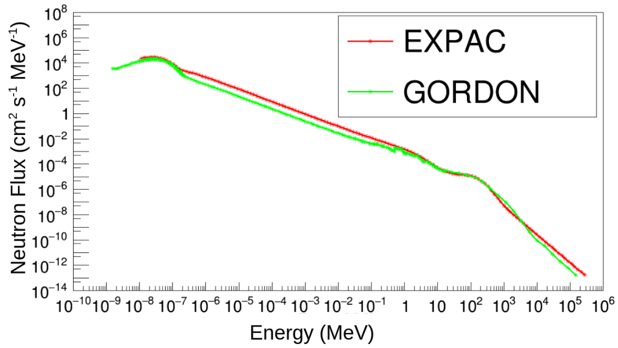

FIGURE 1. Flux distribution calculated by EXPAC Simulation [8, 10, 11] (red) and Gordon Model [7] (light green). Location and time details: Latitude : 42.28^0 N, Longitude : 48.18^0 E , Altitude: 0 m. Date:14/01/2015

numerous analytical functions with parameters whose numerical values were fitted to reproduce the results of the extensive-air-shower simulations performed by the Particle and Heavy Ion Transport code System [9]. EXPAC calculates the atmospheric cosmic-ray spectra of subatomic particles, ions up to ^{28}Ni, muons, and photons [8, 10, 11].

In the Gordon model, neutron-flux and energy-spectrum data from five ground-level measurements in North America are considered. An expression to scale the measured neutron flux to other locations has been developed from an exponential attenuation fit to the altitude dependence of the measurements and an expression from the literature for the geomagnetic and solar-activity dependence of neutron-monitor rates [7]. The Gordon model can be used to estimate the neutron flux only. The EXPAC simulation needs location and time details as input, while the Gordon model needs location details. In the software package, we used the EXPAC simulation for calculating neutron, proton, and photon fluxes, while using the Gordon model for neutron fluxes. We used two models for neutron-flux estimation since the neutrons dominate by a significant margin, and so uncertainties in the neutron flux are the dominant flux uncertainties.

Cross-section libraries

The cross-section library is needed to calculate the activation. We considered the reactions involving the Ar isotopes and neutrons, protons, and photons as projectiles in the software package. The following datasets are used in the calculation to generate the cross-section. The nuclear libraries added are TALYS [12], Japanese Nuclear Data Library (JENDL) [13], Medium Energy Nuclear Data Library (MENDL) [14], and Evaluated Nuclear Data File (ENDF). Except for the neutron resonance region, the ENDF-library estimates are based on nuclear-model predictions and adjusted to experimental results. In the neutron resonance region, the priority is directly given to experimental data [15]. ACTIVIA and INCL are the other two packages used for cross-section calculation. ACTIVIA is a model-based C++ package. With the combination of semi-empirical formulæ, developed by Silberberg and Tsao, and data tables based on experimental results, ACTIVIA calculates cross-sections. To obtain the cross-section library, we used the parameterisations from Silberberg and Tsao [16]. The Liège Intra Nuclear Cascade model (INCL) is a Monte Carlo event generator for nuclear reactions induced by nucleons, pions, or light ions. The model can predict reaction cross-sections, partial cross-sections for any reaction channel, particle correlations, and other quantities [17].

RESULTS

Figure 2 shows the different cross-sections of the ^{40}Ar(n,*)^{37}Ar and ^{40}Ar(n,*)^{3}H reactions as functions of the energy of the projectile neutron. The ^{37}Ar production cross-sections are scaled based on the measurements reported in Ref. [18], which compared calculated production yields to values measured at a neutron beam at the LANSCE facility. The scaling factors used for ACTIVIA, MENDL, TALYS, and INCL are 2.83, 0.326, 0.666, and 0.653, respectively. The application of scaling factors reduces the difference between the nuclear libraries. We used raw cross-section data for all reactions except the ^{40}Ar(n,*)^{37}Ar reaction.

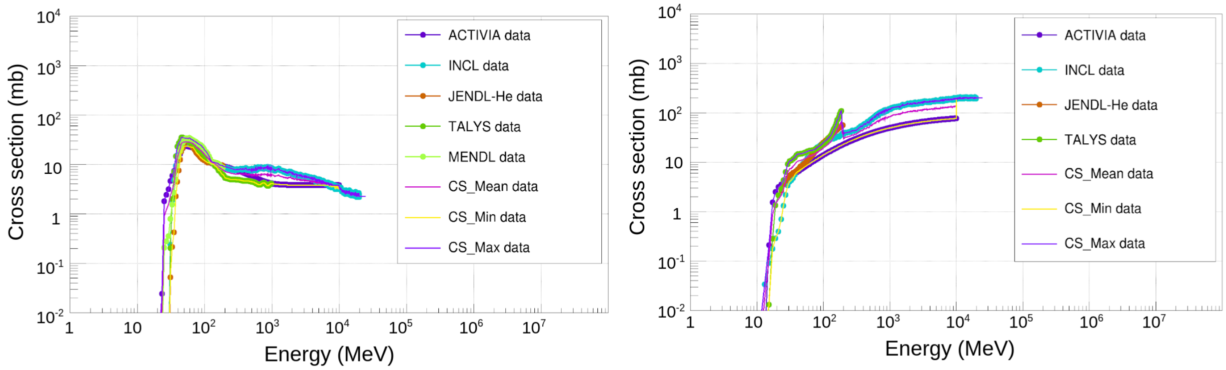

FIGURE 2. Left: different cross-section estimates for the ^{40}Ar(n,*)^{37}Ar reaction as a function of the neutron energy. The scaling factors of cross-section data sets are taken from Ref. [18]. **Right:** different cross-section estimates for the ^{40}Ar(n,*)^{3}H reaction as a function of the neutron energy.

TABLE I. Induced Activity of ^{37}Ar and ^{3}H due to the given reactions. The EXPAC Simulation is used to evaluate the flux.

Reactions	UAr flown [mBq/kg]	UAr Shipped [mBq/kg]	Reactions	UAr flown [mBq/kg]	UAr Shipped [mBq/kg]
^{40}Ar(n,*)^{37}Ar	$1.38^{+0.46}_{-0.47}$	$0.22^{+0.05}_{-0.07}$	^{40}Ar(n,*)^{3}H	$0.08^{+0.05}_{-0.05}$	$0.27^{+0.12}_{-0.10}$
^{36}Ar(n,*)^{37}Ar	$0.35^{+0.09}_{-0.10}$	$0.04^{+0.003}_{-0.01}$	^{36}Ar(n,*)^{3}H	$(6.5^{+3.8}_{-3.9}) \times 10^{-6}$	$(22^{+8.0}_{-4.9}) \times 10^{-6}$
^{40}Ar(p,*)^{37}Ar	$0.46^{+0.20}_{-0.20}$	$0.05^{+0.02}_{-0.02}$	^{40}Ar(p,*)^{3}H	$0.02^{+0.01}_{-0.01}$	$0.05^{+0.02}_{-0.01}$
^{40}Ar(g,*)^{37}Ar	$0.07^{+0.01}_{-0.01}$	$0.01^{+0.0002}_{-0.002}$	^{40}Ar(g,*)^{3}H	$(10.4^{+4.5}_{-4.5}) \times 10^{-5}$	$(40^{+7.8}_{-0.39}) \times 10^{-5}$

The uncertainties on the cross-sections are determined as functions of energy from the maximum variations between the various curves shown in Figure 2. The contribution to the induced activity (IA) from the flux uncertainty is estimated from the variations of the IA between the different flux models.

In order to calculate the induced activity of DS-50 UAr, which can then be compared to data, we need to reconstruct the complete history of the DS-50 UAr from its extraction to the detector site. The DS-50 UAr was transported in two batches from Colorado: a first batch of 141.7 kg by ship and a second batch of 141.7 kg by airplane. The transportation history includes a list of locations specified by latitude, longitude, and altitude, as well as the time when the target sample entered the location and when it left. By road, the different racks of UAr reached Fermilab, where it underwent purification. The UAr was carried to Chicago after that. In the case of UAr transported to Europe by ship, the UAr was transported to Montreal by road and shipped from there to Genoa, Italy. After that, it was carried by road to LNGS. In the case of UAr transported to Europe by plane, from Chicago to Milan, the UAr flew with a stop at Frankfurt, Germany. From Milan to LNGS, it was transported by road.

Uncertainties in the transportation history arise due to unknown details of the target's paths and timing, such as those related to details of the path that a shipping company may have taken. Extreme assumptions in elevation changes between known points are examined to evaluate the effects of these uncertainties on the total activation yield. The software package calculates the nominal activation yields with nominal transportation histories, nominal cross-section values, and the average of both flux models. The uncertainty of the activation yield is determined by varying these three inputs independently by their uncertainties.

The flux uncertainty contributes from 5–15% of the total uncertainty in the induced-activity calculation. In the ^{37}Ar and ^{3}H IA calculations of UAr transported by plane, cross-section uncertainty contributes approximately 40%. In the case of UAr transported by ship, the cross-section uncertainty contributes about 57% (69%) of the total uncertainty of the ^{37}Ar (^{3}H) activity calculation. In the case of UAr transported by airplane, transportation uncertainty contributes approximately 48% (56%) in the case of ^{37}Ar (^{3}H). For UAr shipped, the transportation uncertainty contributes 30% (20%) for ^{37}Ar (^{3}H).

Table I shows the induced activity of ^{37}Ar and ^{3}H due to some major reactions. The fast-neutron interaction of ^{40}Ar and the thermal-neutron interaction of ^{36}Ar contribute a significant fraction of the ^{37}Ar IA. The proton and photon interactions of ^{40}Ar also have a significant role in the ^{37}Ar IA calculation. The half-life of ^{37}Ar is shorter than the exposure time at the overseas level. Therefore, the induced activity of ^{37}Ar in the UAr transported by ship is less than the case of UAr transported by plane. The fast neutron interaction of ^{40}Ar contributes a major fraction of the ^{3}H induced activity. The induced activity of ^{3}H in the UAr transported by ship is greater than that of the UAr transported by plane. Table II shows the total induced activity of ^{37}Ar and ^{3}H computed using the Activation Calculation software package. We considered only cosmic-ray-neutron flux in the calculation because it dominates over secondary neutrons.

TABLE II. Total Induced Activity of ^{37}Ar and ^{3}H, computed for the 16 kg (141.7 kg) of UAr transported by plane (ship)

Radioactive isotopes	UAr flown [mBq/kg]	UAr Shipped [mBq/kg]	Total Activity [mBq/kg]
^{37}Ar	$2.33^{+0.66}_{-0.64}$	$0.33^{+0.10}_{-0.06}$	$0.53^{+0.11}_{-0.09}$
^{3}H	$0.10^{+0.06}_{-0.06}$	$0.33^{+0.11}_{-0.14}$	$0.30^{+0.10}_{-0.13}$

Conclusions

Using the Activation Calculation Software we developed, we estimated the induced activity of ^{37}Ar and ^{3}H isotopes of DS-50 UAr. The ^{37}Ar has a total activity of $0.53^{+0.11}_{-0.09}$ mBq/kg and ^{3}H has a total activity of $0.30^{+0.10}_{-0.13}$ mBq/kg in DS50 UAr. We leave the comparison of these results with DS-50 data to future work.

ACKNOWLEDGMENTS

We thank the Pacific Northwest National Laboratory for the valuable discussions during this work. We acknowledge the support from the DarkSide Collaboration and the suggestions from the collaboration during the project.

REFERENCES

1. S. Cebrián, "Cosmogenic activation of materials," Int. J. Mod. Phys. A **32**, 1743006 (2017), arXiv:1708.07449 [nucl-ex].
2. P. Agnes *et al.* (DarkSide), "Results from the first use of low radioactivity argon in a dark matter search," Phys. Rev. D **93**, 081101 (2016), [Addendum: Phys.Rev.D 95, 069901 (2017)], arXiv:1510.00702 [astro-ph.CO].
3. J. Billard, M. Boulay, S. Cebrián, L. Covi, G. Fiorillo, A. Green, J. Kopp, B. Majorovits, K. Palladino, F. Petricca, L. Roszkowski, and M. Schumann, "Direct detection of dark matter—APPEC committee report*," Rept. Prog. Phys. **85**, 056201 (2022), arXiv:2104.07634 [hep-ex].
4. J. Cooley *et al.*, "Report of the Topical Group on Particle Dark Matter for Snowmass 2021," (2022), arXiv:2209.07426 [hep-ph].
5. P. Agnes *et al.* (DarkSide-20k), "Separating ^{39}Ar from ^{40}Ar by cryogenic distillation with Aria for dark-matter searches," Eur. Phys. J. C **81**, 359 (2021).
6. T. Sato *et al.*, "Development of PARMA: PHITS-based Analytical Radiation Model in the Atmosphere," Radiat. Res. **170**, 244–259 (2008).
7. M. Gordon *et al.*, "Measurement of the flux and energy spectrum of cosmic-ray induced neutrons on the ground," IEEE Transactions on Nuclear Science **51**, 3427–3434 (2004).
8. T. Sato, "Analytical model for estimating the zenith angle dependence of terrestrial cosmic ray fluxes," PLoS ONE **11** (2016), 10.1371/journal.pone.0160390.
9. T. Sato *et al.*, "Particle and Heavy Ion Transport code System, PHITS, version 2.52," J. Nucl. Sci. Technol. **50**, 913–923 (2013).
10. T. Sato, "Analytical model for estimating terrestrial cosmic ray fluxes nearly anytime and anywhere in the world: extension of PARMA/EXPACS," PLoS ONE **10** (2015), 10.1371/journal.pone.0144679.
11. "What is EXPACS?" `http://phits.jaea.go.jp/expacs/main-up-eng.htm`.
12. A. J. Koning *et al.*, "TENDL: complete nuclear data library for innovative nuclear science and technology," Nucl. Data Sheets **155**, 1–55 (2019).
13. J. Katakura, "Development of JENDL decay and fission yield data libraries," Nuclear Data Sheets **118**, 104–107 (2014).
14. Y. N. Shubin, V. P. Lunev, A. Y. Konobeyev, and A. I. Dityuk, "Cross-section library MENDL-2 to study activation and transmutation of materials irradiated by nucleons of intermediate energies," report INDC(CCP) 385 (International Atomic Energy Agency, 1995).
15. B. Pritychenko, "Calculations of astrophysical reaction rates using ENDF/B-VIII.0 library," Nuclear Data Sheets **167**, 76–107 (2020).
16. J. Back and Y. Ramachers, "ACTIVIA: calculation of isotope production cross-sections and yields," Nucl. Instrum. Meth. A **586**, 286–294 (2008), arXiv:0709.3472 [nucl-ex].
17. "INCL general features," `http://irfu.cea.fr/dphn/Spallation/general.html`.
18. R. Saldanha *et al.*, "Cosmogenic production of ^{39}Ar and ^{37}Ar in argon," Physical Review C **100** (2019), 10.1103/physrevc.100.024608.